ADVANCED FUNCTIONAL MATERIALS
www.afm-journal.de

www.MaterialsViews.com

Gated Mesoporous SiO_2 Nanoparticles Using K^+-Stabilized G-Quadruplexes

*Zhanxia Zhang, Fuan Wang, Yang Sung Sohn, Rachel Nechushtai, and Itamar Willner**

The K^+-induced formation of G-quadruplexes provides a versatile motif to lock or unlock substrates trapped in the pores of mesoporous SiO_2 nanoparticles, MP-SiO_2 NPs. In one system, the substrate is locked in the MP-SiO_2 NPs by K^+-ion-stabilized G-quadruplex units, and the pores are unlocked by the elimination of K^+ ions using Kryptofix [2.2.2] (KP) or 18-crown-6-ether (CE) from the G-quadruplexes. In the second system, the substrate is locked in the pores by means of K^+-stabilized aptameric G-quadruplex/thrombin units. Unlocking of the pores is triggered by the dissociation of the aptamer/thrombin complexes through the KP- or CE-mediated elimination of the stabilizing K^+ ions. In the third system, duplex DNA units lock the pores of MP-SiO_2 NPs, and the release of the entrapped substrate is stimulated by the K^+-ion-induced dissociation of the duplex caps through the formation of the K^+-stabilized G-quadruplexes. The latter system is further implemented to release the anti-cancer drug, doxorubicin, in the presence of K^+ ions, from the MP-SiO_2 NPs. Preliminary intracellular experiments reveal that doxorubicin-loaded MP-SiO_2 NPs lead to effective death of breast cancer cells.

1. Introduction

Mesoporous SiO_2 nanoparticles, MP-SiO_2 NPs, attract substantial interest as high-surface-area materials for the entrapment and controlled release of substrates.[1] Different applications of MP-SiO_2 NPs were suggested, including drug delivery,[2] imaging[3] and catalysis.[4] The functionalization of the pores of MP-SiO_2 NPs with stimuli-responsive caps allows the development of "smart" NPs for the controlled release of entrapped substrates by external triggers. Different stimuli, such as pH,[5] redox reagents,[6] optical,[7] thermal[8] and enzymes[9] were used as triggers to unlock the functional gates blocking the pores. Recently, functional nucleic acids were implemented to block the pores of MP-SiO_2 NPs.[10] For example, i-motif nucleic acids were used to cap the pores, and the pH-stimulated dissociation of the i-motif units to random-coil single strands was used to unlock the pores.[11] Similarly, duplex nucleic acid structures were used to block the pores, and their cleavage by exonuclease III or nicking enzymes enabled the release of the pore-entrapped substrates, including the release of an anti-cancer drug, camptothecin.[12] Also, the pores of MP-SiO_2 NPs were locked with nucleic acid nanostructures that, in the presence of appropriate stimuli (e.g., biomarkers), generated catalytic DNAzyme units that hydrolyzed the caps. This led to the unlocking of the pores and to the release of entrapped substrates, including the release of the anti-cancer drug, doxorubicin.[13]

Guanosine-rich nucleic acids are known to self-assemble in the presence of metal ions, such as K^+ ions, into G-quadruplex nanostructures.[14] Several functions of K^+-stabilized G-quadruplexes were reported. For example, the binding of hemin to G-quadruplexes yielded a catalytically active DNAzyme that mimics the functions of horseradish peroxidase (HRP),[15] and the system was broadly applied to develop different sensing platforms[16] and logic gate systems.[17] Similarly, G-rich aptamer sequences were reported to self-assemble into K^+-stabilized G-quadruplex structures upon binding to substrates, e.g., thrombin.[18] Also, K^+-stabilized hemin/G-quadruplex DNAzymes were found to catalyze the oxidation of thiols to disulfides[19] or to mimic the NADH peroxidase and NADH oxidase.[20]

The switchable, stimuli-triggered reconfiguration of DNA structures is a further subject of research interest. For example, the pH-induced switchable transitions of i-motif structures to random-coil single strands,[11,21] or the metal-ion-driven formation of duplex DNA structures and their separation by ligands that eliminate the ions (e.g., T-Hg^{2+}-T/cysteine)[22] were reported as means to reversibly reconfigure DNA nanostructures. Such switchable DNA structures were applied to develop DNA machines (e.g., tweezers[23] and walkers),[24] to drive the switchable formation and dissociation of DNA hydrogels,[25] and to control the switchable "ON/OFF" activation of DNAzymes.[26] Recently, the reconfiguration of K^+-ion-stabilized G-quadruplexes was reported. Upon the addition of K^+-ion-binding ligands, such as 18-crown-6-ether (CE) or cryptofix [2.2.2] (KP), the extraction of K^+ ions from the G-quadruplexes by the receptor ligands led to the dissociation of the G-quadruplexes,[27] and the re-addition of K^+ ions regenerated the G-quadruplex structures. The switchable K^+-ion/ligands-stimulated

Dr. Z. Zhang, Dr. F. Wang, Prof. I. Willner
Institute of Chemistry, Center for Nanoscience and Nanotechnology
The Hebrew University of Jerusalem
Jerusalem 91904, Israel
E-mail: willnea@vms.huji.ac.il
Dr. Y. S. Sohn, Prof. R. Nechushtai
Department of Plant and Environmental Sciences
the Wolfson Centre for Applied Structural Biology
The Hebrew University of Jerusalem
Jerusalem 91904, Israel

DOI: 10.1002/adfm.201400939

formation and dissociation of G-quadruplexes was applied to construct switchable DNA hydrogels that undergo reversible gel-to-solution transitions, and to assemble "ON/OFF" switchable DNAzyme systems.[28] In the present study, we introduce the switchable formation and dissociation of G-quadruplexes associated with MP-SiO_2 NPs as a means to unlock the pores of the NPs and to stimulate the controlled release of pore-entrapped substrates. Since the intracellular concentration of K^+ ions is in the range of 60~80 mM, the K^+-ion-induced formation of G-quadruplexes may provide a general route to unlock DNA-capped mesoporous SiO_2 NPs, thus leading to the release of entrapped drugs.

2. Results and Discussion

The MP-SiO_2 NPs were synthesized according to a reported method.[11] The NPs exhibited a diameter of ca. 0.4 μm (Figure S1, Supporting Information). BET measurement indicated a surface area of 1290.3 m^2/g, and a pore diameter of ca. 3.2 nm (Figure S2, Supporting Information). **Figure 1**(A) depicts the first system to stimulate the controlled release of rhodamine B, RhB, from the pores of MP-SO_2 NPs by switchable G-quadruplex units. Aminosiloxane-functionalized MP-SiO_2 NPs were modified with the nucleic acid (**1**) that includes the G-rich sequence capable of forming the G-quadruplex. In the absence of K^+ ions, the strand (**1**) exists in a random coil configuration that allows the loading of the pores with RhB substrate. These NPs were loaded with RhB, and subsequently, the RhB-loaded NPs were subjected to K^+ ions. This resulted in the reconfiguration of strand (**1**) into the K^+-stabilized G-quadruplex structure (**1a**) that locked the pores. The MP-SiO_2 NPs were extensively washed to remove any residual RhB units that bound to the unlocked exterior domains of the NPs. The G-quadruplex-locked MP-SiO_2 NPs were, then, subjected to the ligand kryptofix [2.2.2] (KP), or to the crown ether, 18-crown-6-ether (CE). The receptor ligands-mediated extraction of K^+ ions from the G-quadruplexes led to the dissociation of the G-quadruplexes, resulting in the unlocking of the pores and the release of RhB. The release of RhB was quantitatively assayed by analyzing aliquot samples of the system via collection of the MP-SiO_2 NPs and probing the fluorescence of the released RhB. Figure 1(B) depicts the fluorescence spectra generated upon the release of RhB from 10 mg of MP-SiO_2 NPs

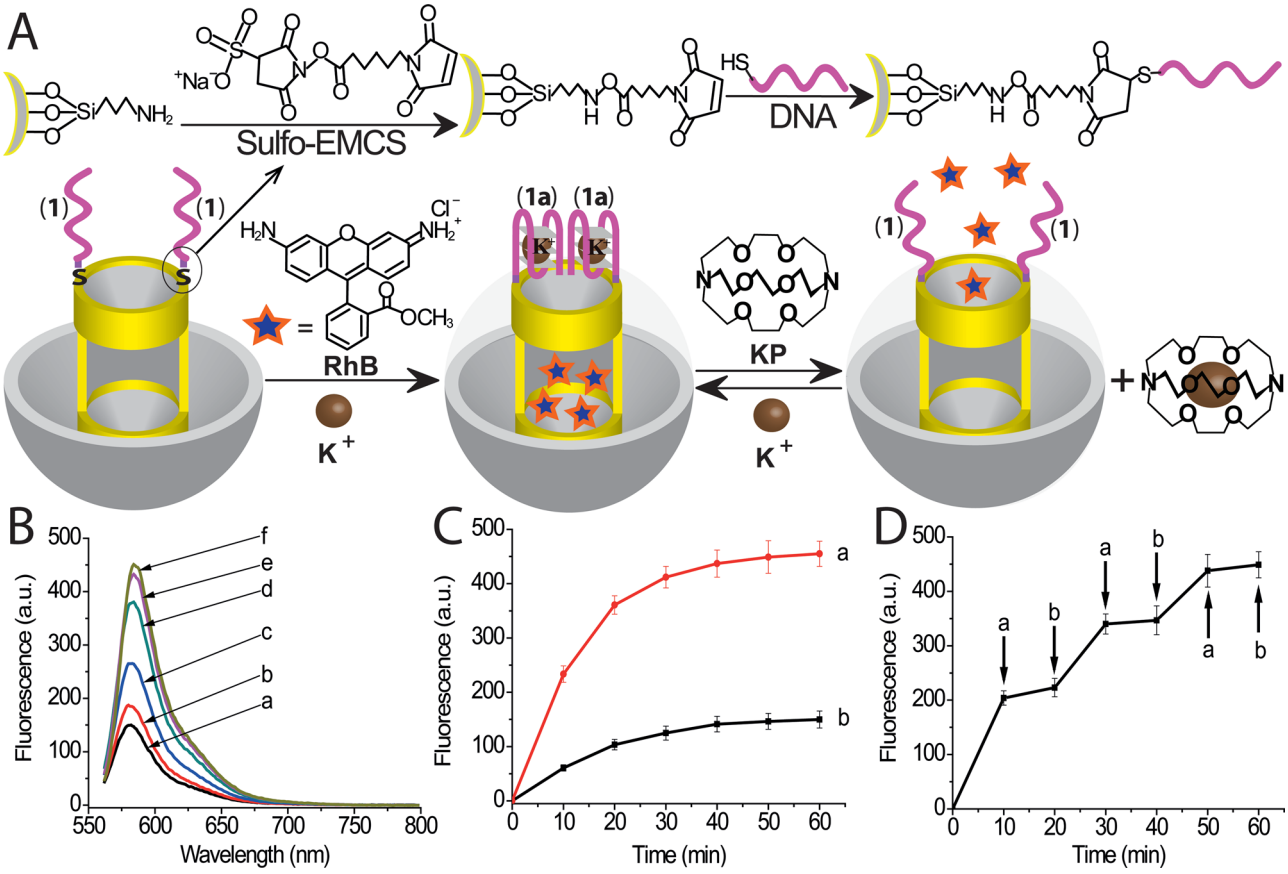

Figure 1. A) Synthesis of the rhodamine B (RhB)-entrapped mesoporous silica nanoparticles, MP-SiO_2 NPs, using K^+-ion-stabilized G-quadruplexes (**1a**) as gates, and the kryptofix [2.2.2] (KP)-triggered dissociation of the gates, stimulating the release of RhB. The sequential treatment of the system with KP and K^+ ions, leads to "ON/OFF" switchable release of RhB. B) Fluorescence spectra corresponding to the released RhB upon subjecting the MP-SiO_2 NPs (10 mg) to different concentrations of KP: a) 0 mM, b) 0.5 mM, c) 1 mM, d) 5 mM, e) 10 mM and f) 50 mM, for a fixed time-interval of 60 minutes. C) Time-dependent fluorescence changes upon releasing RhB from 10 mg RhB-loaded MP-SiO_2 NPs: a) upon treatment of the MP-SiO_2 NPs with 10 mM KP; b) without KP. D) Switchable release of RhB from the MP-SiO_2 NPs upon cyclic unlocking and locking of the pores: a) unlocking of the pores with 10 mM KP; b) re-locking of the pores with 10 mM K^+ ions.

for a fixed time-interval of 60 minutes, using different concentrations of KP (for the analogous experiment using CE as triggering stimulus see Figure S3, Supporting Information). As the concentration of KP increases, the fluorescence spectra of the released RhB are intensified. This is consistent with the fact that at higher concentrations of KP, the elimination of K^+ ions from the G-quadruplex units is more effective, resulting in the improved unlocking of the pores, and the enhanced release of RhB encapsulated in the pores of MP-SiO_2 NPs. One might realize that even in the presence of K^+ ions a small amount of RhB is released from the NPs to the solution. This might originate from the leakage of RhB from imperfectly-blocked pores of MP-SiO_2 NPs (for further explanation that this leakage occurs from imperfect sites, vide infra). Figure 1(C), **curve (a),** depicts the time-dependent fluorescence changes upon subjecting the RhB-loaded NPs to a fixed amount of KP, 10 mM. The time-dependent fluorescence changes correspond to the release of RhB from the pores. The fluorescence intensity increases with time, and it levels-off to a constant value that corresponds to the total amount of the released RhB. The total amount of RhB trapped in the pores of the MP-SiO_2 NPs was estimated to be ca. 15.3 μmole/g MP-SiO_2 NPs (for the determination of the loading see experimental section). From the saturated fluorescence intensity observed upon the KP-triggered release of RhB, and using an appropriate calibration curve, we estimate that the amount of released RhB is ca. 2.3 μmole/g MP-SiO_2 NPs. That is, only ca. 15% of the loaded RhB was released from the NPs. The incomplete release of RhB is attributed to the partial trapping of the dye in nanoporous domains that perturb the diffusional release of the dye from the pores. Figure 1(C), **curve (b)**, depicts the time-dependent fluorescence change observed upon allowing the RhB-loaded MP-SiO_2 NPs to release RhB without adding the KP ligand. In the absence of K^+ ions, the pores are unlocked, and therefore the release of RhB is expected. After ca. 60 minutes, the fluorescence intensity levels-off to a constant value that is ca. 3-fold lower than the fluorescence of the released RhB in the presence of 10 mM of KP. It should be noted that even after long time-intervals, the saturated fluorescence value of RhB released from the NPs, in the absence of KP, does not change. Thus, the inefficient release of RhB (ca. 0.8 μmole/g MP-SiO_2 NPs) occurs from imperfectly locked pores, that allow the release of RhB even in the absence of KP. By subjecting the RhB-loaded MP-SiO_2 NPs to cyclic stimuli of KP and K^+ ions, the switchable "ON" and "OFF" release of RhB from the pores was demonstrated, Figure 1(D). Treatment of the MP-SiO_2 NPs with KP unlocked the pores, and triggered the release of RhB. The addition of K^+ ions re-locked the pores. These results imply that the KP ligand not only triggered "ON" the release of RhB, but the sequential treatment of the NPs with KP/K^+-ion allowed the dose-controlled release of RhB from the NPs.

The second G-quadruplex-regulated system for the switchable controlled release of substrates (e.g., RhB) from mesoporous SiO_2 NPs has implemented aptameric G-quadruplex/substrate units as locks of the pores of the NPs. This method is depicted in **Figure 2**(A) using the thrombin/aptamer complexes, thrombin/G-quadruplex (**2a**), as locking units.[29] The aminosiloxane-functionalized MP-SiO_2 NPs were modified with the nucleic acid (**2**) that included the anti-thrombin aptamer sequence. These NPs were loaded with RhB, and the pores were locked by the addition of K^+ ions and thrombin. The resulting thrombin/G-quadruplex complex units locked the pores, and the RhB associated with non-pore domains was washed off. The loading of RhB associated with the aptameric G-quadruplex/thrombin-locked NPs corresponded to ca. 19.8 μmole/g MP-SiO_2 NPs. The subsequent treatment of the NPs with KP eliminated the K^+ ions from the complexes, resulting in the dissociation of the G-quadruplexes and the separation of the aptamer/thrombin complexes. The resluting unlocked pores allowed the release of RhB. Figure 2(B) depicts the fluorescence spectra of RhB released from the RhB-loaded MP-SiO_2 NPs, 10 mg, upon interaction with different concentrations of KP for a fixed time-interval of 90 minutes (for the analogous experiment using CE as triggering stimulus see Figure S4, Supporting Information). As the concentration of KP increases, the fluorescence of RhB is intensified, consistent with a more efficient release of RhB from the pores. Figure 2(C), **curve (a)**, shows the time-dependent fluorescence changes upon the release of RhB from the RhB-loaded NPs, 10 mg, in the presence of KP, 10 mM. A time-dependent intensity increase in the fluorescence of the released RhB is observed, and it levels-off after ca. 90 minutes. Knowing the saturation level of the released RhB, and using an appropriate calibration curve, we estimated that the amount of released RhB was ca. 3.4 μmole/g MP-SiO_2 NPs, upon the KP-stimulated unlocking of the pores. That is, ca. 17% of the loaded RhB was released from the pores. Figure 2(C), **curve (b)**, shows the time-dependent fluorescence changes upon the leakage of RhB from the imperfectly capped aptameric G-quadruplex/thrombin-blocked pores, in the absence of KP. The fluorescence of the released RhB is ca. 4-fold lower (ca. 0.8 μmole/g MP-SiO_2 NPs) than the RhB released in the presence of 10 mM KP. This might originate from the non-blocked exterior domains of the NPs.

The third configuration to unlock the MP-SiO_2 NPs by means of K^+-stabilized G-quadruplexes is presented in **Figure 3**(A). The method makes use of the fact that duplex DNA structures block the pores, while single-stranded nucleic acids lack blocking functions.[13] Accordingly, the aminosiloxane-modified MP-SiO_2 NPs were functionalized with the nucleic acid (**3**). The NPs were loaded with RhB, and the substrate was locked in the pores by the hybridization of the nucleic acid (**4**) with the surface-anchored DNA strand (**3**). The nucleic acid (**4**) included, however, the G-quadruplex sequence that was part of the hybridization domain, and partially composed of the single-stranded domain (**I**). The loading of RhB on the (**3**)/(**4**)-blocked pores was estimated to be ca. 13.2 μmole/g MP-SiO_2 NPs. In the presence of K^+ ions, the G-rich sequence associated with strand (**4**) assembles into a G-quadruplex. The residual duplex domain between strands (**3**) and (**4**) is, however, energetically insufficient to retain the duplex structure. This results in the separation of the K^+-ion-stabilized G-quadruplex of strand (**4a**), and the release of RhB substrate encapsulated in the pores of MP-SiO_2 NPs. Treatment of the system with KP or CE separated the G-quadruplex by eliminating the K^+ ions, and the free strand (**4**) re-hybridized with strand (**3**) to block the pores. Figure 3(B) shows the fluorescence spectra of RhB released into the solution, upon subjecting the RhB-loaded NPs to variable concentrations of K^+ ions, for a fixed time-interval

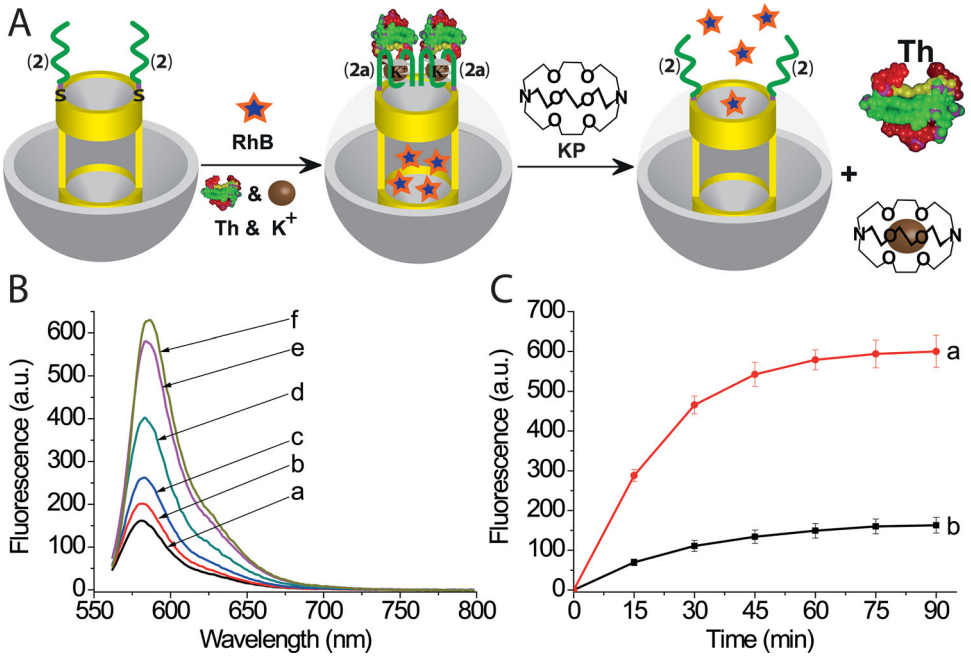

Figure 2. A) Synthesis of the rhodamine B (RhB)-entrapped MP-SiO_2 NPs, using K^+-ion-stabilized thrombin (Th) aptamer G-quadruplex/thrombin (**2a**) units as gates, and the kryptofix [2.2.2] (KP)-triggered dissociation of the gates, stimulating the release of RhB. B) Fluorescence spectra corresponding to the released RhB upon subjecting 10 mg MP-SiO_2 NPs to different concentrations of KP: a) 0 mM, b) 0.1 mM, c) 0.5 mM, d) 1 mM, e) 5 mM and f) 10 mM, for a fixed time-interval of 90 minutes. C) Time-dependent fluorescence changes upon releasing RhB from 10 mg (**2a**)-capped MP-SiO_2 NPs: a) upon treatment of the MP-SiO_2 NPs with 10 mM KP; b) without KP.

of 60 minutes. As expected, as the concentration of K^+ ions is higher, the release of RhB substrate from the pores is more efficient, consistent with the improved unlocking of the pores by the generation of the G-quadruplexes, being separated from the duplex DNA caps. Figure 3(C) depicts the time-dependent fluorescence changes of the released RhB from the MP-SiO_2 NPs upon unlocking the pores by 10 mM K^+ ions. The fluorescence intensity increases with time, and it reaches a saturation value after ca. 60 minutes. From the saturated value of the fluorescence intensity, reached upon the K^+-ion-triggered unlocking of the pores, and using an appropriate calibration curve, we estimate that the amount of released RhB is ca. 1.8 μmole/g MP-SiO_2 NPs. Figure 3(D) shows the switchable unlocking and locking of the pores by the cyclic interaction of the NPs with K^+ ions and KP, respectively. The K^+ ions unlock the pores, resulting in the release of RhB substrate. The subsequent treatment of the system with KP regenerated the blocked pores. By the cyclic treatment of the NPs with K^+-ion/KP, the switchable unlocking/locking of the pores is demonstrated. This latter experiment highlights the possibility to control the dose of the released substrates by means of K^+-ion/KP. Finally, Figure 3(E) reveals the selective unlocking of the (**3**)/(**4**)-capped MP-SiO_2 NPs by K^+ ions. The (**3**)/(**4**)-capped RhB-loaded NPs were treated with Li^+, Na^+ and NH_4^+ ions, and the release of RhB from NPs in the presence of the different ions was compared to the releasing system stimulated by K^+ ions. The release of RhB in the presence of Li^+, Na^+ and NH_4^+ ions is inefficient (ca. 2.5-fold lower than the K^+-ion-stimulated release of RhB), and is very similar to the background release of RhB from the imperfectly blocked pores. These results are consistent with the fact that only K^+ ions effectively and cooperatively stabilize the G-quadruplex structures.[30]

The third configuration outlined in Figure 3(A) has specific advantages for intracellular controlled drug release applications. The content of K^+ ions in cells is ca. 80 mM, a value that suggests the potential intracellular unlocking of the pores and the K^+-ion-driven release of the drug encapsulated in the pores. Accordingly, the (**3**)-functionalized MP-SiO_2 NPs were loaded with the anti-cancer drug doxorubicin, Dox, and the pores were locked with the (**3**)/(**4**) duplex units. **Figure 4**(A) shows the fluorescence spectra of the released doxorubicin upon subjecting the Dox-loaded MP-SiO_2 NPs to variable concentrations of K^+ ions, for a fixed time-interval of 60 minutes. As the concentration of K^+ ions increases the content of the released doxorubicin increases (higher fluorescence), consistent with the improved K^+-ion-stimulated unlocking of the pores through the dissociation of the (**3**)/(**4**) duplex structures, and the separation of the K^+-ion-stabilized G-quadruplexes. Figure 4(B) depicts the time-dependent release of doxorubicin from the (**3**)/(**4**)-capped Dox-loaded MP-SiO_2 NPs in the presence of 10 mM K^+ ions, **curve (a)**, and in the absence of K^+ ions, **curve (b)**. The K^+-ion-stimulated release of doxorubicin is ca. 2.5-fold higher as compared to the background release of doxorubicin in the absence of K^+ ions. It should be noted that the release of doxorubicin in the absence of K^+ ions levels off to a saturation value after ca. 60 minutes and the content of the released doxorubicin never reaches the amount released by the K^+-ion-stimulated unlocking of the pores. This background fluorescence change is attributed to the release of doxorubicin from imperfectly blocked pores by (**3**)/(**4**) duplex caps.

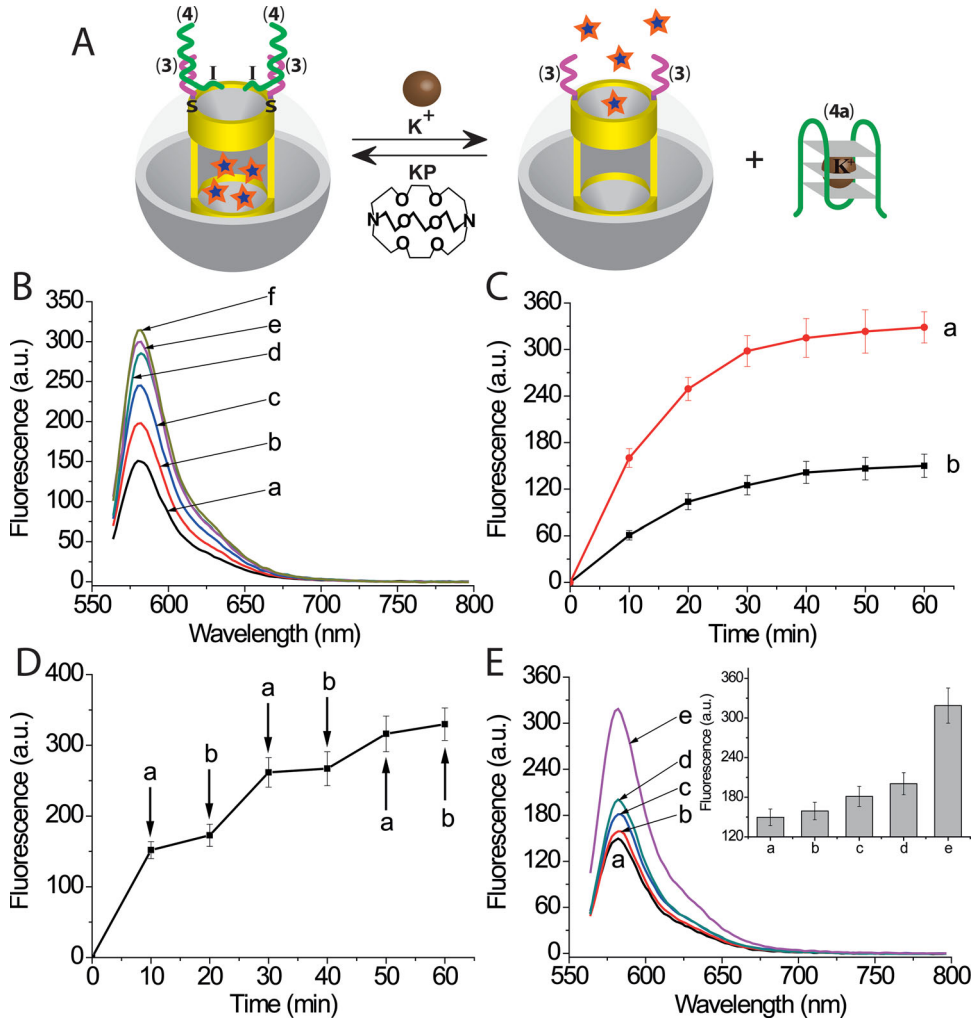

Figure 3. A) Synthesis of the rhodamine B (RhB)-entrapped MP-SiO_2 NPs, using (**3**)/(**4**) duplex units as gates, and the K^+-ion-triggered dissociation of the gates, stimulating the release of RhB. The sequential treatment of the system with K^+ ions and KP, leads to "ON/OFF" switchable release of RhB. B) Fluorescence spectra corresponding to the released RhB upon subjecting the MP-SiO_2 NPs (10 mg) to different concentrations of K^+ ions: a) 0 mM, b) 0.5 mM, c) 1 mM, d) 5 mM, e) 10 mM and f) 50 mM, for a fixed time-interval of 60 minutes. C) Time-dependent fluorescence changes upon releasing RhB from 10 mg (**3**)/(**4**)-capped MP-SiO_2 NPs: a) with 10 mM K^+ ions; b) without K^+ ions. D) Switchable release of RhB from the MP-SiO_2 NPs upon cyclic a) unlocking of the pores with 10 mM K^+ ions, and b) re-locking of the pores with 10 mM KP. E) Fluorescence spectra corresponding to the released RhB from 10 mg (**3**)/(**4**)-capped MP-SiO_2 NPs after a fixed time-interval of 60 minutes: a) Without added ions; b) In the precence of 10 mM Li^+ ions; c) In the precence of 10 mM NH_4^+ ions; d) In the precence of 10 mM Na^+ ions; e) In the precence of 10 mM K^+ ions. Inset: selectivity presented in the form of bars of fluorescence intensity.

The effect of Dox-loaded MP-SiO_2 NPs on normal breast epithelial cells (MCF-10a) and breast cancer cells (MDA-MB-231) was examined. In order to image the MP-SiO_2 NPs in the cells, the unloaded MP-SiO_2 NPs or Dox-loaded NPs were labeled with fluorescein isothiocyanate (FITC) (see experimental section). As a first experiment we examined the cytotoxicity of unloaded FITC-labeled MP-SiO_2 NPs (Figure S5, Supporting Information). No cytotoxic effect of the MP-SiO_2 NPs was observed. **Figure 5**(A) shows the confocal microscopy images corresponding to the normal breast cells MCF-10a, panel I, and breast cancer cells MDA-MB-231, panel II, treated with the FITC-labeled Dox-loaded MP-SiO_2 NPs (for a fixed time-interval of 18 hours). Clearly, the fluorescein signal as well as the doxorubicin fluorescence signal are substantially higher in the cancer cells as compared to the normal cells, implying that endocytosis of the MP-SiO_2 NPs into cancer is more efficient than into the normal breast cells. Although the origin for this improved endocytosis of the MP-SiO_2 NPs into cancer cells is not understood, we find that this property apparently leads to the substantial increased death of cancer cells, as compared to normal cells. Figure 5(B) depicts the percentage of cancer cell death (70%) as compared to normal cells death (40%) upon their treatment with the Dox-loaded MP-SiO_2 NPs for a fixed time-interval of 18 hours. Although these experiments are at a preliminary stage, they are encouraging, since they demonstrate enhanced activities on the cancer cells. Further experiments that implement the Dox-loaded MP-SiO_2 NPs functionalized with specific anti-cancer cell antibodies or the capping of the

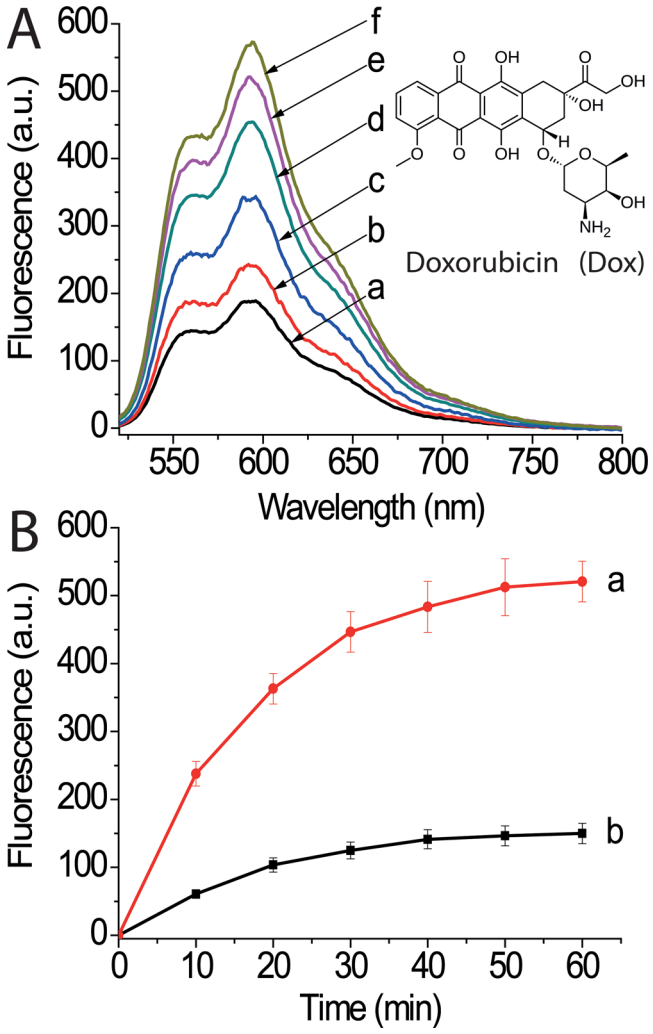

Figure 4. A) Release of doxorubicin (Dox) using K^+ ions as activators for opening the (**3**)/(**4**)-capped MP-SiO_2 NPs. Fluorescence spectra corresponding to the released Dox upon subjecting the MP-SiO_2 NPs (10 mg) to different concentrations of K^+ ions: a) 0 mM, b) 0.5 mM, c) 1 mM, d) 5 mM, e) 10 mM and f) 50 mM, for a fixed time-interval of 60 minutes. B) Time-dependent fluorescence changes observed upon the release of Dox from the MP-SiO_2 NPs: a) upon treatment of the MP-SiO_2 NPs with 10 mM K^+ ions; b) without K^+ ions.

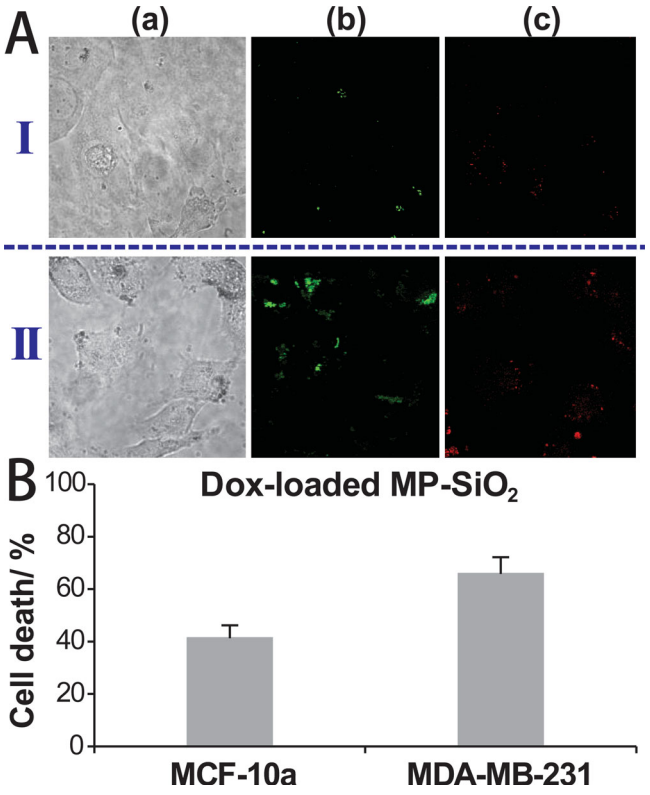

Figure 5. Cytotoxicity of doxorubicin (Dox)-loaded FITC-labeled MP-SiO_2 NPs in normal breast cells (MCF-10a) and breast cancer cells (MDA-MB-231). A) Semi-Confocal Microscopy (Nikon TE2000 microscope equipped with opti-grid) images corresponding to the FITC-labeled Dox-loaded MP-SiO_2 NPs: panel I, normal breast cells (MCF-10a); panel II, breast cancer cells (MDA-MB-231) where a) corresponds to the phase image of the cells. b) The green fluorescence of the FITC chromphore. c) The red fluorescence of the Dox-loaded NPs. Note that the co-locolization of the red Dox-fluorescence with the green FITC-fluorescence corresponds to ca. 40%. This probably originates from the release of the drug to the cytoplasm during the twelve hours of interaction of the NPs with the cells. B) The percentage of cell death compared with the control cells without treatment is obtained by cell viability measurements using alamar blue assay after treatment with Dox-loaded FITC-labeled MP-SiO_2 NPs in normal breast cells (MCF-10a) and breast cancer cells (MDA-MB-231).

NPs with duplex nucleic acids of increased stabilities, could further enhance the selectivity of the functionalized NPs towards the cancer cells.

3. Conclusions

The present study has introduced a new method to lock and unlock substrates trapped in the pores of MP-SiO_2 NPs by means of G-quadruplexes. One system has involved the locking of the substrate in the pores by means of K^+-ion-stabilized G-quadruplexes as capping units, and the unlocking of the pores by the kryptofix [2.2.2]- or 18-crown-6-ether-mediated elimination of the K^+ ions, leading to the dissociation of the capping G-quadruplexes. In the second system the locking of the pores was achieved by the implementation of a K^+-ion-stabilized aptameric G-quadruplex/protein complexes (the anti-thrombin G-quadruplex aptamer/thrombin complexes) as locking units. Similarly, the pores were unlocked by the kryptofix [2.2.2]- or 18-crown-6-ether-stimulated uptake of the stabilizing K^+ ions processes, leading to the dissociation of the G-quadruplex/thrombin complex caps. The third system has applied duplex DNA structures as the capping units to lock the pores. The K^+-ion-triggered separation of the duplex structures through the formation of K^+-ion-stabilized G-quadruplexes by one of the duplex strand led to the unlocking of the pores and to the release of the entrapped substrate. The third configuration reveals relevance for nanomedicine since cellular K^+-ion levels that correspond to 80 mM are capable to unlock the pores and to release the encapsulated drugs. Indeed, preliminary experiments have demonstrated that MP-SiO_2 NPs loaded with the anti-cancer drug, doxorubicin,

and capped by duplex nucleic acids, undergo effective endocytosis into cancer cells. The intracellular K^+ ions trigger the opening of the pores, thus leading to the effective death of cancer cells. The unlocking of drug-loaded MP-SiO_2 NPs by means of K^+-ion-induced formation of G-quadruplexes might be further developed by entrapping other anti-cancer drugs in the pores of the MP-SiO_2 NPs, and by further modifying the MP-SiO_2 NPs with specific anti-cancer antibodies that could target the drug-carrying NPs to specific cancer cells. The discovery that K^+-ion-stabilized G-quadruplexes lock substrates in the pores of MP-SiO_2 NPs might spark, however, several new research directions: (i) The binding of hemin to G-quadruplexes results in catalytically active DNAzyme units, and thus, catalyzed chemical transformations in the pores may be envisaged. (ii) Different fluorophores reveal enhanced luminescence properties upon their binding to G-quadruplexes, e.g., Zn(II)-protoporphyrin IX or Tb^{3+} ions. These fluorescent MP-SiO_2 NPs might be used for bioimaging intracellular nano-environments and for following the localized release of substrates at specific target sites.

4. Experimental Section

Reagents and Materials: Tetraethyl orthosilicate (TEOS), (3-aminopropyl)-triethoxysilane (APTES), fluorescein isothiocyanate (FITC) and rhodamine B (RhB) were purchased from Aldrich. Hexadecyltrimethylammonium bromide (CTAB), 4-(2-hydroxyethyl) piperazine-1-ethanesulfonic acid sodium salt (HEPES), doxorubicin hydrochloride (Dox), 18-crown-6-ether (CE) and thrombin (Th, from bovine plasma) were purchased from Sigma. N-(ε-Maleimidocaproyloxy) sulfosuccinimide ester (Sulfo-EMCS) was purchased from Pierce Biotechnologies. Kryptofix [2.2.2] (KP) was purchased from Acros. All chemicals were of analytical grade and were used as received without any further purification. Ultrapure water from a NANOpure Diamond (Barnstead Int., Dubuque, IA) source was used throughout the experiments. All the DNA strands were purchased from Integrated DNA Technologies. (Coralville, IA). The sequences of the nucleic acids are as follows:

(**1**) 5′-HS$(CH_2)_6$ TTAGGGTTAGGGTTAGGGTTAGGG-3′

(**2**) 5′-HS$(CH_2)_6$ TGGTTGGTGTGGTTGG-3′

(**3**) 5′-HS$(CH_2)_6$ ACCCTAACCCT-3′

(**4**) 5′-GGGTTAGGGTTAGGGTTAGGG-3′

Instruments: Fluorescence emission measurements were recorded using a Cary Eclipse Device (Varian, Inc.). Rhodamine B (RhB) and doxorubicin (Dox) were excited at 554 nm and 500 nm, respectively. UV-vis absorption spectra were recorded with a Shimadzu UV-2401 spectrophotometer. Scanning electron microscopy (SEM) images were recorded on a Tecnai F20 G2 (FEI Co.) using an accelerating voltage of 200 kV. Surface area and pore size of the MP-SiO_2 NPs were determined using a Nova 1200e Brunauer-Emmett-Teller (BET) meter (Quantachrome Instruments).

Synthesis of Mesoporous Silica Nanoparticles (MP-SiO_2 NPs): Amino-functionalized MP-SiO_2 NPs were synthesized according to a previously reported procedure.[11] The collected MP-SiO_2 NPs were washed with large volumes of distilled water and ethanol using a centrifuge at 6000 rpm for 3 minutes. To remove the CTAB template, the SiO_2 NPs were refluxed for 16 hours in a solution composed of HCl (37%, 1 ml) and ethanol (80 ml). The resulting NPs were extensively washed with distilled water and ethanol, respectively. Finally, to remove the remaining solvents from the pores, the amino-functionalized, CTAB-free, MP-SiO_2 NPs were dried under vacuum at 75 °C for 12 hours.

Loading the Dye and Capping the Pores: A mixture consisting of monodispersed amino-functionalized MP-SiO_2 NPs solution was prepared by placing 10 mg MP-SiO_2 NPs in 950 μl HEPES buffer (10 mM, pH 7.0) followed by the sonication of the mixture for 1 hour. The resulting solution was mixed with 50 μl of sulfo-EMCS (10 mg ml^{-1}) and allowed to react for 30 minutes. To remove excess of sulfo-EMCS, the MP-SiO_2 NPs were collected using a centrifuge at 6000 rpm for 3 minutes, and the NPs were re-dissolved in 950 μl HEPES buffer (10 mM, pH 7.0). The purified MP-SiO_2 NPs were reacted with freshly reduced and purified thiolated oligonucleotides (**1**), (**2**), or (**3**) (100 μl, 1 mM), and incubated for 2 hours (The as-provided thiolated nucleic acids, protected in the form of disulfide, were reduced with dithiothreitol (DTT), 0.1 M. The resulting thiolated nucleic acids were separated from excess of DTT using a MicroSpin G-25 Column). The loading of the different nucleic acids (**1**), (**2**) or (**3**) on the respective MP-SiO_2 NPs was determined as follows. The nucleic acid at a known concentration was reacted with the functionalized NPs, and the resulting particles were collected by centrifugation at 6000 rpm for 3 minutes. The concentration of the unreacted nucleic acids in the solution was evaluated by absorbance spectroscopy. By the subtraction of the content of unreacted nucleic acids from the content of nucleic acids added to the reaction media, the loading of the nucleic acids on the MP-SiO_2 NPs was estimated to be: (**1**) 1.8 μmol g^{-1}, (**2**) 2.1 μmol g^{-1}, and (**3**) 2.5 μmol g^{-1} of MP-SiO_2 NPs. Subsequently, the RhB was loaded in the different MP-SiO_2 NPs. The loading of RhB in the K^+-ion-stabilized G-quadruplex-capped pores was evaluated as follow: A mixture of 0.9 ml consisting of 850 μl HEPES buffer (10 mM, pH 7.0), and 50 μl aqueous 10 mM RhB solution was prepared. MP-SiO_2 NPs, 10 mg, were added to the mixture that was allowed to react while shaking for 12 hours. Afterwards, 100 μl of a KCl solution, 100 mM, were added to the mixture to cap the pores while forming the G-quadruplexes, and the mixture was incubated for 2 hours. For the K^+-ion-stabilized thrombin aptamer G-quadruplex/thrombin-capped system, the nucleic acid (**2**)-modified MP-SiO_2 NPs, 10 mg, were introduced into 750 μl of HEPES buffer (10 mM, pH 7.0), and subsequently, 50 μl of RhB solution (10 mM) was added to the mixture, and the system was incubated for 12 hours. Afterwards, 100 μl thrombin solution (2.5 μM) and 100 μl KCl solution (100 mM) were added to the resulting mixture, and the system was allowed to react for 2 hours. For the preparation of the (**3**)/(**4**)-capped MP-SiO_2 NPs system, the (**3**)-modified MP-SiO_2 NPs, 10 mg, were introduced into the mixture consisting of 850 μl HEPES buffer (10 mM, pH 7.0) and 50 μl RhB solution (10 mM), and the system was incubated for 12 hours. Afterwards, 100 μl of (**4**) (1 mM) was added to the resulting mixture, and the system was allowed to react for 2 hours. Then, the loading of substrates in the pores for the three different systems was accomplished by collecting the loaded NPs of the different systems by centrifugation at 6000 rpm for 3 minutes. Finally, the particles were washed at least six times with HEPES buffer (10 mM, pH 7.0) until no background fluorescence was observed. The contents of RhB in the washing solution were determined, and these correspond to RhB that is physically adsorbed on the non-pore domains of the NPs. Knowing the content of RhB present in the solution after the primary NPs precipitation process, and knowing the amounts of RhB eliminated by the washing procedure from the different systems, the total content of residual non-bound RhB of the different systems was evaluated. As the initial content of RhB added for the loading of the NPs is known, the difference between the two values corresponds to the loading of the MP-SiO_2 NPs with RhB. Using this procedure, the loading of the K^+-ion-stabilized G-quadruplex (**1a**)-capped system corresponded to 15.3 μmole/g, of the aptameric G-quadruplex/thrombin (**2a**)-capped system corresponded to 19.8 μmole/g, and the loading of the duplex (**3**)/(**4**)-capped MP-SiO_2 NPs corresponded to 13.2 μmole/g of MP-SiO_2 NPs. The (**3**)/(**4**)-capped doxorubicin (Dox)-loaded MP-SiO_2 NPs were prepared by the introduction of 10 mg (**3**)-functionalized MP-SiO_2 NPs into 800 μl HEPES buffer (10 mM, pH 7.0). To the mixture 200 μl Dox aqueous solution (10 mM) was added and the mixture was allowed to interact, while shaking, for 12 hours. Subsequently, 100 μl of (**4**) (1 mM) were added to the mixture, and the system was allowed to react for

2 hours. The resulting (**3**)/(**4**)-capped Dox-loaded MP-SiO_2 NPs were centrifuged at 6000 rpm for 3 minutes and the particles were washed at least six times to remove the physically-adsorbed Dox. The loading of Dox in the MP-SiO_2 NPs was determined as described for RhB, and it corresponded to 27.6 μmole/g of MP-SiO_2 NPs.

Release of the Dye: The release of RhB from RhB-loaded MP-SiO_2 NPs capped with the K^+-ion-stabilized G-quadruplex units (**1a**) or capped with the K^+-ion-stabilized G-quadruplex/thrombin (**2a**) units were analyzed as follows: The respective RhB-loaded MP-SiO_2 NPs, 10 mg, were introduced into 900 μl HEPES buffer (10 mM, pH 7.0), and the mixture was divided into five samples. Subsequently, 20 μl of aqueous solution of different concentrations of KP or CE were added to the samples that were allowed to react for a fixed time-interval of 60 minutes for the (**1a**)-capped system, and 90 minutes for the (**2a**)-capped system. The resulting mixtures were centrifuged, and the MP-SiO_2 NPs were separated. The fluorescence spectra of the supernatant clear solutions were then recorded. For the time-dependent release of RhB from the respective systems, a similar procedure was applied while subjecting the NPs, for different time-intervals, at a fixed concentration of KP. For the release of RhB from the (**3**)/(**4**)-capped MP-SiO_2 NPs, the RhB-loaded NPs were introduced into 900 μl of water, and the mixture was divided into five samples, 180 μl each. KCl aqueous solutions of different concentrations were added to the mixture, and the total volume of each sample was completed to 200 μl. The samples were allowed to react for a fixed time-interval of 60 minutes. Subsequently, the NPs were collected (centrifugation at 6000 rpm for 3 minutes) and the fluorescence spectra of RhB released into the solutions were recorded. The time-dependent release of Dox from the NPs was probed by adapting a similar procedure as described before, using a fixed concentration of KCl (10 mM).

Cell Experiments: To image the MP-SiO_2 NPs in the cells, the amino-functionalized MP-SiO_2 NPs were prepared in the presence of fluorescein isothiocyanate, FITC, (TEOS, 9 mmole; APTES, 38 μmole; FITC, 1 μmole).[31] We find that the loading of the NPs by doxorubicin (Dox), and the release of Dox, upon unlocking the pores are unaffected by the fluorescein modifier. For the microscopy, normal breast cells (MCF-10a), breast cancer cells (MDA-MB-231) were planted on microscopic slides attached to perforated tissue culture 3 cm plate and were incubated with 0.6 mg/ml of MP-SiO_2 NPs in growth medium for 6 hours. After intensive washing with DMEM-Hepes and quenching of extracellular fluorescence using trypan blue, the fluorescence of FITC was measured by epi-fluorescence microscopy (Nikon TE2000 microscope) equipped with opti-grid. Magnification was 600, oil objective was a (Plan Apo) 60/1.40 NA. Image analysis was done by image-J, Volocity programs. For the cell viability, MCF-10a and MDA-MB-231 cells were planted at a density of 2×10^4 cells/well in 96-well plates. After 12 hours, the cells were incubated with MP-SiO_2 samples for 18 hours. After intensive washing of the cells with growth medium, cell viability was determined with the fluorescent redox probe, alamar blue. The fluorescence of alamar blue was recored on a plate-reader (Tecan Safire) after 1 hour of incubation at 37 °C ($\lambda_{ex} = 560$ nm; $\lambda_{em} = 590$ nm).

Supporting Information

Supporting Information is available from the Wiley Online Library or from the author.

Acknowledgements

This research is supported by NanoSensoMach ERC Advanced Grant No. 267574 under the EC FP7/2007–2013 program. The research is performed under the auspices of the MINERVA Center for Biohybrid Complex Systems.

Received: March 23, 2014
Revised: April 27, 2014
Published online: July 3, 2014

[1] a) Z. Li, J. C. Barnes, A. Bosoy, J. F. Stoddart, J. I. Zink, *Chem. Soc. Rev.* **2012**, *41*, 2590–2605; b) J. E. Lee, N. Lee, T. Kim, J. Kim, T. Hyeon, *Acc. Chem. Res.* **2011**, *44*, 893–902.

[2] a) J. L. Vivero-Escoto, I. I. Slowing, B. G. Trewyn, V. S.-Y. Lin, *Small* **2010**, *6*, 1952–1967; b) F. Tang, L. Li, D. Chen, *Adv. Mater.* **2012**, *24*, 1504–1534.

[3] a) M. Liong, S. Angelos, E. Choi, K. Patel, J. F. Stoddart, J. I. Zink, *J. Mater. Chem.* **2009**, *19*, 6251–6257; b) J. E. Lee, N. Lee, H. Kim, J. Kim, S. H. Choi, J. H. Kim, T. Kim, I. C. Song, S. P. Park, W. K. Moon, T. Hyeon, *J. Am. Chem. Soc.* **2010**, *132*, 552–557.

[4] a) H. Song, R. M. Rioux, J. D. Hoefelmeyer, R. Komor, K. Niesz, M. Grass, P. Yang, G. A. Somorjai, *J. Am. Chem. Soc.* **2006**, *128*, 3027–3037; b) A. Dandapat, D. Jana, G. De, *ACS Appl. Mat. Interfaces* **2009**, *1*, 833–840.

[5] a) H. Meng, M. Xue, T. Xia, Y.-L. Zhao, F. Tamanoi, J. F. Stoddart, J. I. Zink, A. E. Nel, *J. Am. Chem. Soc.* **2010**, *132*, 12690–12697; b) R. Liu, Y. Zhang, X. Zhao, A. Agarwal, L. J. Mueller, P. Feng, *J. Am. Chem. Soc.* **2010**, *132*, 1500–1501; c) Q. Yang, S. Wang, P. Fan, L. Wang, Y. Di, K. Lin, F.-S. Xiao, *Chem. Mater.* **2005**, *17*, 5999–6003.

[6] a) T. D. Nguyen, Y. Liu, S. Saha, K. C.-F. Leung, J. F. Stoddart, J. I. Zink, *J. Am. Chem. Soc.* **2007**, *129*, 626–634; b) J.-T. Sun, J.-G. Piao, L.-H. Wang, M. Javed, C.-Y. Hong, C.-Y. Pan, *Macromol. Rapid Commun.* **2013**, *34*, 1387–1394; c) Z. Zhang, D. Balogh, F. Wang, R. Tel-Vered, N. Levy, S. Y. Sung, R. Nechushtai, I. Willner, *J. Mater. Chem. B* **2013**, *1*, 3159–3166.

[7] a) E. Aznar, R. Casasus, B. Garcia-Acosta, M. D. Marcos, R. Martinez-Manez, F. Sancenon, J. Soto, P. Amoros, *Adv. Mater.* **2007**, *19*, 2228–2231; b) Q. Yuan, Y. Zhang, T. Chen, D. Lu, Z. Zhao, X. Zhang, Z. Li, C.-H. Yan, W. Tan, *ACS Nano* **2012**, *6*, 6337–6344; c) N. K. Mal, M. Fujiwara, Y. Tanaka, T. Taguchi, M. Matsukata, *Chem. Mater.* **2003**, *15*, 3385–3394.

[8] a) X. Yang, X. Liu, Z. Liu, F. Pu, J. Ren, X. Qu, *Adv. Mater.* **2012**, *24*, 2890–2895; b) Z. Zhang, L. Wang, J. Wang, X. Jiang, X. Li, Z. Hu, Y. Ji, X. Wu, C. Chen, *Adv. Mater.* **2012**, *24*, 1418–1423.

[9] a) C. Coll, L. Mondragon, R. Martinez-Manez, F. Sancenon, M. D. Marcos, J. Soto, P. Amoros, E. Perez-Paya, *Angew. Chem. Int. Ed.* **2011**, *50*, 2138–2140; b) K. Patel, S. Angelos, W. R. Dichtel, A. Coskun, Y.-W. Yang, J. I. Zink, J. F. Stoddart, *J. Am. Chem. Soc.* **2008**, *130*, 2382–2383; c) A. Bernardos, L. Mondragon, E. Aznar, M. D. Marcos, R. Martinez-Manez, F. Sancenon, J. Soto, J. M. Barat, E. Perez-Paya, C. Guillem, P. Amoros, *ACS Nano* **2010**, *4*, 6353–6368.

[10] a) Y. Zhang, Q. Yuan, T. Chen, X. Zhang, Y. Chen, W. Tan, *Anal. Chem.* **2012**, *84*, 1956–1962; b) E. Climent, L. Mondragón, R. Martínez-Máñez, F. Sancenón, M. D. Marcos, J. R. Murguía, P. Amorós, K. Rurack, E. Pérez-Payá, *Angew. Chem. Int. Ed.* **2013**, *52*, 8938–8942; c) L. Chen, J. Di, C. Cao, Y. Zhao, Y. Ma, J. Luo, Y. Wen, W. Song, Y. Song, L. Jiang, *Chem. Commun.* **2011**, *47*, 2850–2852.

[11] C. Chen, F. Pu, Z. Huang, Z. Liu, J. Ren, X. Qu, *Nucleic Acids Res.* **2011**, *39*, 1638–1644.

[12] a) Z. Zhang, D. Balogh, F. Wang, S. Y. Sung, R. Nechushtai, I. Willner, *ACS Nano* **2013**, *7*, 8455–8468; b) R. Duan, F. Xia, L. Jiang, *ACS Nano* **2013**, *7*, 8344–8349.

[13] Z. Zhang, D. Balogh, F. Wang, I. Willner, *J. Am. Chem. Soc.* **2013**, *135*, 1934–1940.

[14] a) D. Sen, W. Gilbert, *Nature* **1990**, *344*, 410–414; b) J. T. Davis, *Angew. Chem. Int. Ed.* **2004**, *43*, 668–698; c) A. Ambrus, D. Chen, J. Dai, T. Bialis, R. A. Jones, D. Yang, *Nucleic Acids Res.* **2006**, *34*, 2723–2735.

[15] a) P. Travascio, Y. Li, D. Sen, *Chem. Biol.* **1998**, *5*, 505–517; b) P. Travascio, P. K. Witting, A. G. Mauk, D. Sen, *J. Am. Chem. Soc.* **2001**, *123*, 1337–1348; c) V. Pavlov, Y. Xiao, R. Gill, A. Dishon, M. Kotler, I. Willner, *Anal. Chem.* **2004**, *76*, 2152–2156; d) F. Wang, R. Orbach, I. Willner, *Chem. Eur. J.* **2012**, *18*, 16030–16036.

[16] a) J. Tang, L. Hou, D. Tang, B. Zhang, J. Zhou, G. Chen, *Chem. Commun.* **2012**, *48*, 8180–8182; b) S. Shimron, F. Wang, R. Orbach, I. Willner, *Anal. Chem.* **2012**, *84*, 1042–1048; b) F. Wang, C.-H. Lu, X. Liu, L. Freage, I. Willner, *Anal. Chem.* **2014**, *86*, 1614–1621.

[17] a) B. Shlyahovsky, Y. Li, O. Lioubashevski, J. Elbaz, I. Willner, *ACS Nano* **2009**, *3*, 1831–1843; b) M. Moshe, J. Elbaz, I. Willner, *Nano Lett.* **2009**, *9*, 1196–1200; c) J. Zhu, L. Zhang, T. Li, S. Dong, E. Wang, *Adv. Mater.* **2013**, *25*, 2440–2444; d) F. Wang, C.-H. Lu, I. Willner, *Chem. Rev.* **2014**, *114*, 2881–2941.

[18] D. M. Tasset, M. F. Kubik, W. Steiner, *J. Mol. Biol.* **1997**, *272*, 688–698.

[19] a) E. Golub, R. Freeman, I. Willner, *Anal. Chem.* **2013**, *85*, 12126–12133; b) E. Sharon, E. Golub, A. Niazov-Elkan, D. Balogh, I. Willner, *Anal. Chem.* **2014**, *86*, 3153–3158.

[20] E. Golub, R. Freeman, I. Willner, *Angew. Chem. Int. Ed.* **2011**, *50*, 11710–11714.

[21] a) K. Gehring, J. L. Leroy, M. Guéron, *Nature* **1993**, *363*, 561–565; b) D. Collin, K. Gehring, *J. Am. Chem. Soc.* **1998**, *120*, 4069–4072; c) H. Liu, Y. Xu, F. Li, Y. Yang, W. Wang, Y. Song, D. Liu, *Angew. Chem. Int. Ed.* **2007**, *46*, 2515–2517.

[22] a) Y. Miyake, H. Togashi, M. Tashiro, H. Yamaguchi, S. Oda, M. Kudo, Y. Tanaka, Y. Kondo, R. Sawa, T. Fujimoto, T. Machinami, A. Ono, *J. Am. Chem. Soc.* **2006**, *128*, 2172–2173; b) Z.-G. Wang, J. Elbaz, F. Remacle, R. D. Levine, I. Willner, *P. Natl. Acad. Sci. USA* **2010**, *107*, 21996–22001; c) M. Stobiecka, A. A. Molinero, A. Chałupa, M. Hepel, *Anal. Chem.* **2012**, *84*, 4970–4978.

[23] a) B. Yurke, A. J. Turberfield, A. P. Mills Jr., F. C. Simmel, J. L. Neumann, *Nature* **2000**, *406*, 605–608; b) J. Elbaz, M. Moshe, I. Willner, *Angew. Chem., Int. Ed.* **2009**, *48*, 3834–3837; c) X. Liang, H. Nishioka, N. Takenaka, H. Asanuma, *ChemBioChem* **2008**, *9*, 702–705; d) J. Elbaz, Z. G. Wang, R. Orbach, I. Willner, *Nano Lett.* **2009**, *9*, 4510–4514.

[24] a) C. Wang, J. Ren, X. Qu, *Chem. Commun.* **2011**, *47*, 1428–1430; b) Z.-G. Wang, J. Elbaz, I. Willner, *Nano Lett.* **2011**, *11*, 304–309; c) X. Liu, A. Niazov-Elkan, F. Wang, I. Willner, *Nano Lett.* **2013**, *13*, 219–225.

[25] a) H. Kang, H. Liu, X. Zhang, J. Yan, Z. Zhu, L. Peng, H. Yang, Y. Kim, W. Tan, *Langmuir* **2011**, *27*, 399–408; b) T. Zhou, P. Chen, L. Niu, J. Jin, D. Liang, Z. Li, Z. Yang, D. Liu, *Angew. Chem., Int. Ed.* **2012**, *51*, 11271–11274; c) W. Guo, X.-J. Qi, R. Orbach, C.-H. Lu, L. Freage, I. Mironi-Harpaz, D. Seliktar, H.-H. Yang, I. Willner, *Chem. Commun.* **2014**, *50*, 4065–4068.

[26] a) S. Shimron, J. Elbaz, A. Henning, I. Willner, *Chem. Commun.* **2010**, *46*, 3250–3252; b) J. Elbaz, S. Shimron, I. Willner, *Chem. Commun.* **2010**, *46*, 1209–1211.

[27] M. A. Aleman-Garcia, R. Orbach, I. Willner, *Chem. Eur. J.* **2014**, *20*, 5619–5624.

[28] C.-H. Lu, X.-J. Qi, R. Orbach, H.-H. Yang, I. Mironi-Harpaz, D. Seliktar, I. Willner, *Nano Lett.* **2013**, *13*, 1298–1302.

[29] a) A. D. Rache, I. Kejnovska, M. Vorlickova, C. Buess-Herman, *Chem. Eur. J.* **2012**, *18*, 4392–4400; b) Z. Zhang, W. Yang, J. Wang, C. Yang, F. Yang, X. Yang, *Talanta* **2009**, *78*, 1240–1245; c) H. Chang, L. Tang, Y. Wang, J. Jiang, J. Li, *Anal. Chem.* **2010**, *82*, 2341–2346.

[30] D. Kong, Y. Ma, J. Guo, W. Yang, H. Shen, *Anal. Chem.* **2009**, *81*, 2678–2684.

[31] C. Chen, J. Geng, F. Pu, X. Yang, J. Ren, X. Qu, *Angew. Chem. Int. Ed.* **2011**, *50*, 882–886.